

A numerical study of the Schrödinger-Newton equation 2: the time-dependent problem

R Harrison, I Moroz and K P Tod
Mathematical Institute
St Giles
Oxford OX1 3LB

October 28, 2018

Abstract

We present a numerical study of the time-dependent SN equations in three dimensions with three kinds of symmetry: spherically symmetric, axially symmetric and translationally symmetric. We find that the solutions show a balance between the dispersive tendencies of the Schrödinger equation and the gravitational attraction from the Poisson equation. Only the ground state is stable, and lumps of probability attract each other gravitationally before dispersing.

1 Introduction

This is the second in a series of papers presenting a numerical study of the Schrödinger-Newton (or SN) equations. In the first ([4]) we reviewed known results on the SN equations and then analysed the linear stability of the spherically-symmetric stationary states. We found that the ground state is linearly stable, in that all the eigenvalues for linear perturbations were purely imaginary, while all the higher states are unstable. The $(n + 1)$ -th state, or equivalently the n -th excited state, has n quadruples $(\lambda, -\lambda, \bar{\lambda}, -\bar{\lambda})$

of complex eigenvalues with nonzero real part. We now want to go further in two directions. On the one hand we shall consider the full nonlinear evolution of the SN equations and on the other we shall move away from spherical symmetry, allowing for two space variables.

In the evolution of spherically-symmetric data we shall find that the picture from linear theory is confirmed: the ground state is stable but slight perturbations of the higher states decay, with probability density escaping off the grid to leave a ‘nugget’ consisting of the ground state rescaled to have total probability less than one and situated at the origin. For more general spherically-symmetric data the picture is confirmed: solutions typically disperse leaving a nugget of rescaled ground state. (By a rescaled ground state we mean the following: if $\psi_0(r)$ is the spatial part of the wave function for the ground state, normalised to have total probability equal to one and with conserved energy \mathcal{E}_0 in the terminology of [4], then $p^2\psi_0(pr)$ with p a positive constant, is a stationary solution with conserved energy $p^3\mathcal{E}_0$ and total probability p .)

We can introduce a new space variable in two ways. We may consider axially-symmetric solutions in 3-dimensions. In this case there are new 3-dimensional stationary states, somewhat analogous to the axially-symmetric solutions of the hydrogen atom, and with nonzero expectation for the angular momentum. These turn out to be unstable under evolution, as one would expect. For the solution most analogous to a pure dipole, the evolution clearly shows the two ‘lumps’ of probability falling from rest into each other and evolving towards the ground state, with some scatter.

Alternatively we may consider translation-invariant solutions in 3-dimensions or equivalently the SN equations in 2+1-dimensions. (Of course the solutions are not normalisable as 3 + 1-dimensional solutions but this is still an interesting problem.) In this case we can find rigidly-rotating stationary states like two lumps of probability rotating around each other. When these are evolved with the time-dependent SN equations they prove to be unstable, so that it is possible to arrange for two lumps of probability to be in orbit around each other at least for a while before they merge.

In summary, the picture that we find is of a system with dispersive tendencies because of the Schrödinger equation and attractive or concentrating tendencies from the gravitational attraction. There appear to be infinitely many stationary states, all of them unstable except for the ground state. General data evolve to leave some residual probability in a rescaled ground

state with the rest of the probability dispersing. Lumps of probability in the initial data can attract each other and even orbit each other but eventually the dispersive tendencies win.

The plan of the paper is as follows. We shall end this Introduction with an analytic result bounding the residual probability left on the grid at late times. In Section 2 we introduce the numerical method which we shall use to evolve the spherically-symmetric SN equations. The results of this evolution are presented in Section 3. In Section 4 we present the results of numerically evolving 3-dimensional axisymmetric solutions and in Section 5 we present the results of numerically evolving the 2-dimensional SN equations.

For the analytic calculation then, suppose that the picture presented above holds in general so that arbitrary initial data evolve to give a scattering solution which disperses to infinity and leaves a rescaled ground state. Then we can obtain a bound on the probability remaining in the ground state provided the initial energy is negative. For suppose the initial value of the conserved energy is \mathcal{E}_I then since this is conserved, we can calculate at late times to find

$$\mathcal{E}_I = \mathcal{E}_S + p^3 \mathcal{E}_0$$

where \mathcal{E}_S is the energy in the scattering solution, which we suppose to be positive, \mathcal{E}_0 is the (negative) energy of the ground state and p is the probability left in the ground state. (The ground state is strongly peaked at the origin so that the cross-term in \mathcal{E}_I is zero.) Taking account of all the signs, if $\mathcal{E}_I < 0$ we can rearrange this to read

$$p^3 > \frac{|\mathcal{E}_I|}{|\mathcal{E}_0|} \tag{1}$$

which is the desired bound.

2 Numerical methods for the spherically-symmetric evolution

Recall from [4] that the SN equations are the system

$$\begin{aligned} i \frac{\partial \psi}{\partial t} &= -\nabla^2 \psi + \phi \psi, \\ \nabla^2 \phi &= |\psi|^2. \end{aligned} \tag{2}$$

In this section and the next, we are concerned only with the spherically-symmetric case and in this case (2) can be simplified as

$$i\frac{\partial u}{\partial t} = -\frac{\partial^2 u}{\partial r^2} + \phi u, \quad (3)$$

$$\frac{\partial^2(r\phi)}{\partial r^2} = \frac{|u|^2}{r}, \quad (4)$$

where $u = r\psi$.

To solve this system, we shall use a Crank-Nicholson method for the time-evolution of the Schrödinger equation and the spectral method of [4] for the Poisson equation. Schematically, this takes the form

$$2i\frac{u^{n+1} - u^n}{\delta t} = -D^2(u^{n+1}) - D^2(u^n) + \phi^{n+1}u^{n+1} + \phi^n u^n, \quad (5)$$

where, with the spectral method of [4], D^2 is the second-derivative matrix for Chebyshev polynomials. The Crank-Nicholson method is second-order accurate in the time and preserves the normalisation of the wave function.

Now we need an iterative method to find ϕ^{n+1} . We write ϕ_k^{n+1} and u_k^{n+1} for the iterates and make the initial choice $\phi_0^{n+1} = \phi^n$, then use the spectral method to solve (5) for u_0^{n+1} , use this in (4) to improve ϕ_0^{n+1} to ϕ_1^{n+1} , and solve (5) to find u_1^{n+1} . This cycle can be repeated until the desired degree of convergence is reached.

The boundary conditions are that u and $r\phi$ should vanish at the origin and the outer edge $r = L$ of the grid. We expect there to be an outgoing flux of probability and we need to prevent it from reflecting back off of the boundary. For this we use the ‘sponges’ of Bernstein et al [2]. The idea is to replace the i on the left-hand-side in (3) by $i + s(r)$ where $s(r)$ is a positive function large (of order one) near the boundary but small close in. We typically use $s(r) = ae^{b(r-L)}$ for constants a and b . By this means the Schrödinger equation is converted to a heat equation near the boundary and the outgoing flux is absorbed.

We can perform various checks on the method outlined here. To check that the sponges are working as desired, we temporarily set $\phi = 0$ and consider the numerical evolution corresponding to the following explicit spherically-

symmetric solution of the zero-potential Schrödinger equation:

$$r\psi = u = \frac{C\sqrt{\sigma}}{(\sigma^2 + 2it)^{\frac{1}{2}}} \left[\exp\left(-\frac{(r - vt - a)^2}{2(\sigma^2 + 2it)} + \frac{ivr}{2} - \frac{iv^2t}{4}\right) - \exp\left(-\frac{(r + vt + a)^2}{2(\sigma^2 + 2it)} - \frac{ivr}{2} - \frac{iv^2t}{4}\right) \right] \quad (6)$$

where C is a normalisation constant (which can be found explicitly). This solution is a spherically-symmetric bump with a Gaussian profile centred initially at $r = a$ and moving radially with velocity v . It both disperses and moves off the grid. Computing it is a test for the Schrödinger evolution, and having it move smoothly off the grid is a test for the sponges. The initial data for the solution (6) will be evolved in the full evolution in Section 3.

Next, we can include a fixed ϕ in (3), dropping (4) and jointly test the Schrödinger evolution and the sponges. Finally, we can test convergence of the method by varying the time step and/or the number of Chebyshev points chosen in the spectral method.

3 Results in the spherically-symmetric case

Having tested the method and the sponges satisfactorily, we evolve the ground state, that is we use as initial data the stationary-state of lowest energy which is known from [6] or [4]. Since this is a stationary state it should evolve with a factor e^{-iEt} and this is just what we find (see figure 1: the phase is linear in time). However if this evolution is continued for a long enough time, numerical errors accumulate and the solution drifts away from the ground state. By Fourier analysing the solution one finds lines in the power spectrum at (approximately) the normal frequencies for a perturbation about the ground state already found by linear perturbation theory in [4]. Thus we really are getting the stable but perturbed ground state. We have also evolved from data which are the ground state with a small perturbation introduced by hand and the picture is the same.

Next we evolve the second spherically-symmetric stationary state taken from [4]. We should expect this also to evolve as a stationary state at least for a while until numerical errors accumulate. What we obtain is shown in figure 2. This shows $|r\psi|$, so that the second state, which has a zero, appears as bimodal. The evolution proceeds as a stationary-state to about

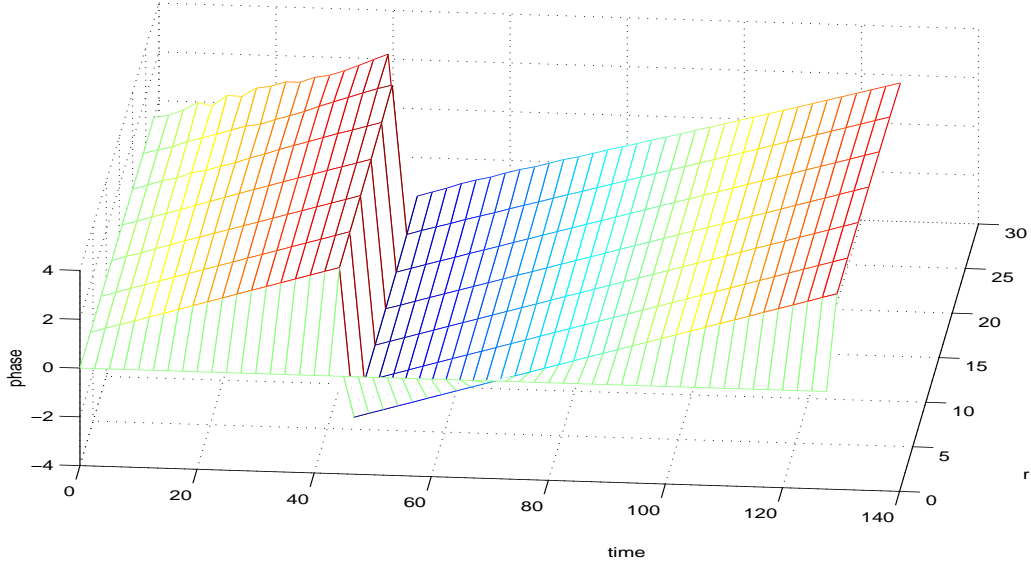


Figure 1: The phase angle of the ground state as a function of time.

$t = 2000$ and then there is a sudden change to a unimodal solution with some oscillation. This we claim is a perturbed and rescaled ground state solution, with total probability less than one.

To support this claim, we have again calculated the power spectrum and find lines at (approximately) the normal frequencies of perturbations about the ground state (to find agreement we need to rescale these frequencies with the factor corresponding to the rescaling of the residual ground state). We can also use the check suggested by equation (1). That is, we calculate both the probability p and the action or conserved energy \mathcal{E} remaining on the grid at time t and compute the bound on p provided by (1). If the argument leading to this bound is correct then these two probabilities should converge on each other and as we see in figure 3 they do. Again, we can evolve from the second state with a small perturbation introduced by hand rather than waiting for the numerical errors to accumulate when the collapse to the ground state is more rapid, or alternatively we can evolve from the second state but with a more stringent tolerance on the iteration determining ϕ , when the collapse takes longer.

Moving on, the decay of the third state is shown in figure 4. The initial state this time has three maxima and evolves for a while as a stationary

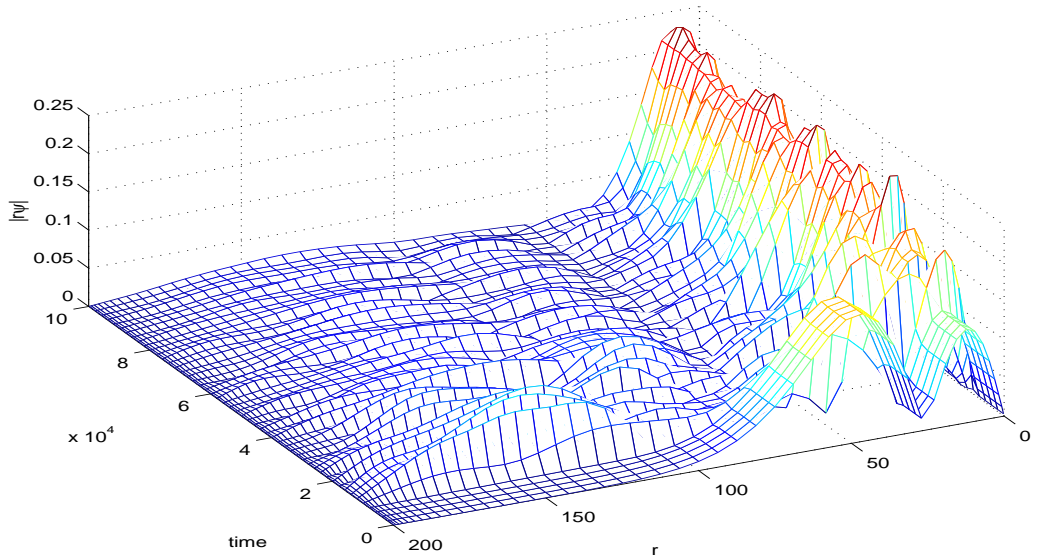


Figure 2: Evolution of second state.

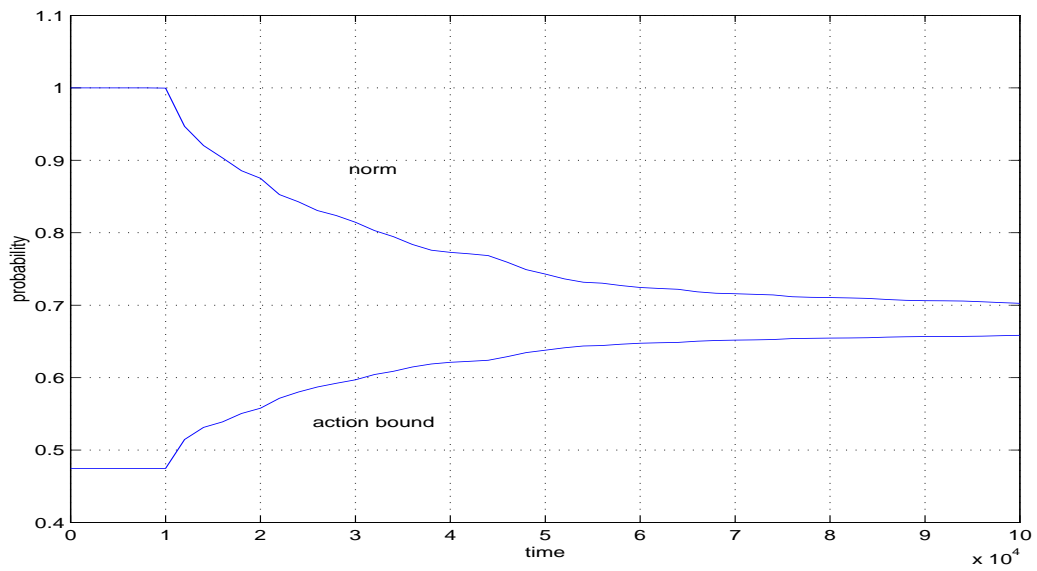


Figure 3: Decay of the second state: the two measures of probability converging

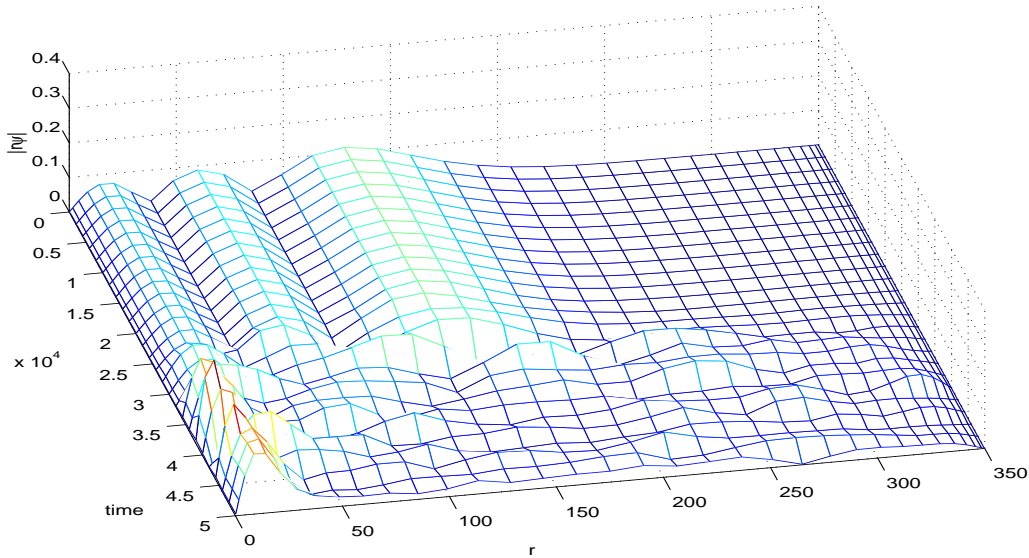


Figure 4: Evolution of third state.

state before collapsing to a rescaled ground state with the emission of some probability to infinity. We have plotted the figure corresponding to figure 3 and we again find convergence.

The picture that emerges from these calculations is of nonlinear instability of all states after the ground state. Each higher state decays to the ground state either by the accumulation of numerical errors or because of an explicitly included perturbation. The end result is a noisy rescaled ground state, noisy because the eigenvalues for perturbation about the ground state are all imaginary.

The other spherically symmetric evolutions which we have calculated are with the initial data furnished by equation (6) with $t = 0$. This is a Gaussian bump centered at $r = a$ with width σ and moving with velocity v . The conserved energy of this data rises with v (because the kinetic energy rises) and with σ (because the particle is more localised). In all cases the solution disperses leaving a rescaled ground state which we can characterise by the probability residing in it. In figures 5, 6 and 7 we plot the residual probability against v , a and σ at different times.

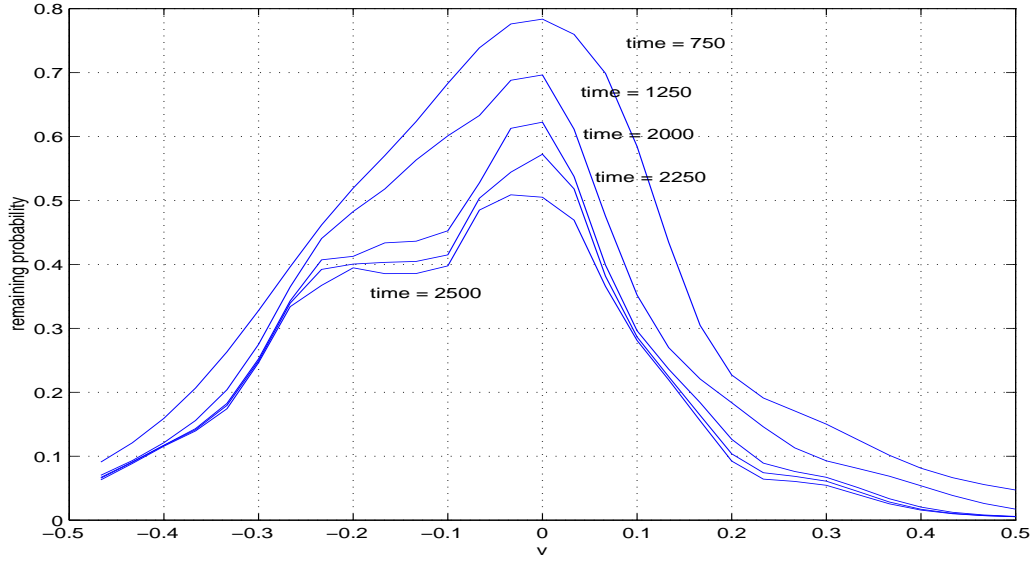


Figure 5: Evolution of Gaussians with varying v : $\sigma = 6$, $a = 50$.

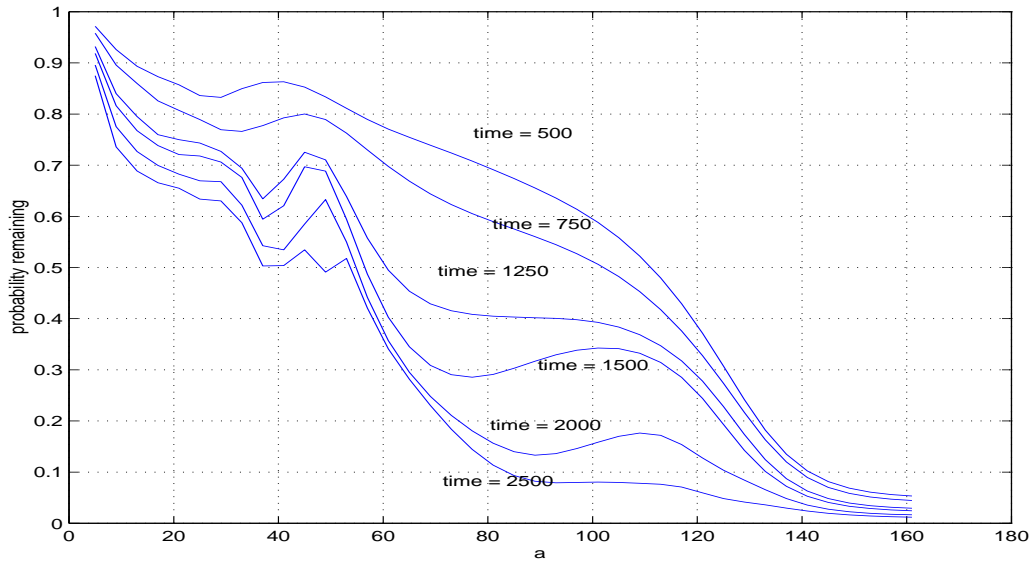


Figure 6: Evolution of Gaussians with varying a : $\sigma = 6$, $v = 0$.

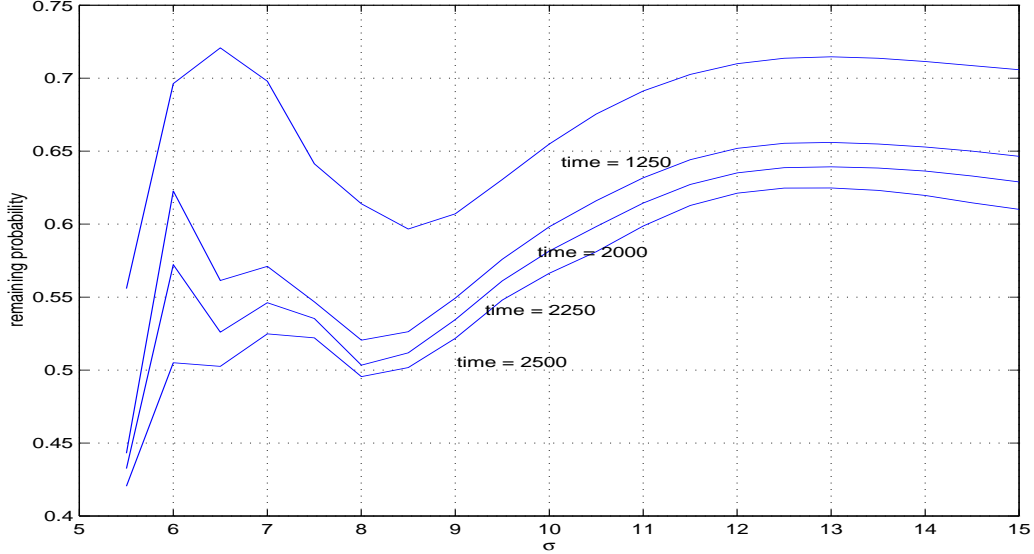


Figure 7: Evolution of Gaussians with varying σ : $v = 0$, $a = 50$.

From figure 5 we see that the residual probability is greatest if the lump is released from rest, but it is easier to trap probability if the initial velocity is ingoing than if it is outgoing. From figure 6 we see that for lumps released from rest, the residual probability is greater if the lump starts closer in, or in other words is more gravitationally bound. From figure 7 we see that reducing σ , which raises the energy, leads to more dispersion.

A key motivation for this set of calculations was the desire to check convergence of the method, and we have done this in a variety of ways. First for the time-step, with a Crank-Nicholson method we expect to have quadratic convergence, and this can be investigated with a Richardson quotient. We suppose that for some variable of interest the calculated value O_h and actual values I are related by

$$O_h \sim I + Ah^k,$$

where the time step size is h , and k is the order of the error, then we can calculate the Richardson quotient:

$$\frac{O_{h_1} - O_{h_3}}{O_{h_2} - O_{h_3}},$$

where h_1, h_2 and h_3 are three different values of the step size. With k known,

this will be a simple function of the h_i and so will provide a check on k . Next for convergence in space we can repeat the calculation with different numbers N of Chebyshev points. For both checks, the results converge as required.

With this calculation we confirm the picture of the SN evolution which we have been claiming: the Schrödinger equation tends to disperse probability but the Newtonian gravitational attraction holds it together; all states after the ground state are unstable and the evolution in general leads to a dispersion of probability to infinity, leaving some residual probability in a rescaled ground state.

4 The axially-symmetric SN equations

In this chapter, we solve the SN equations for an axially-symmetric system in 3 dimensions. The wave-function is now a function of polar coordinates r and θ but is independent of polar angle. We shall first find stationary solutions. These typically have nonzero total angular momentum and include a dipole-like solution which appears to minimise the energy among wave functions which are odd in (the usual) z . We then consider the time-dependent problem. In particular we evolve the dipole-like state, and it turns out to be nonlinearly unstable - the two regions of probability density attract each other and fall together leaving a multiple of the ground state as the evolutions in Section 2 did.

With $u = r\psi$ the system of equations (2) becomes:

$$iu_t = -u_{rr} - \frac{1}{r^2 \sin \theta} (\sin \theta u_\theta)_\theta + \phi u, \quad (7)$$

$$\frac{|u|^2}{r} = (r\phi)_{rr} + \frac{1}{r \sin \theta} (\sin \theta \phi_\theta)_\theta. \quad (8)$$

For stationary solutions, the left-hand-side of (7) is replaced by Eu . Boundary conditions are that $u = 0$ at $r = 0$ and $r = L$, $\phi = 0$ at $r = L$ and finite at $r = 0$, and $u_\theta = 0 = \phi_\theta$ at $\theta = 0$ and $\theta = \pi$.

To find stationary solutions we proceed as follows:

1. take as an initial guess for the potential $\phi = \frac{-1}{(1+r)}$;
2. using this potential solve the time-independent Schrödinger equation;

3. select an eigenfunction in such a way that the procedure will converge to a stationary state (this needs trial and error);
4. calculate the potential due to the chosen eigenfunction;
5. take the new potential to be the one obtained from step 4 above but symmetrised, since we require that ϕ should be symmetric around the $\theta = \frac{\pi}{2}$ (otherwise numerical errors can cause the wave-function to move along the axis);
6. now provided that the new potential does not differ from the previous potential by some fixed tolerance in the norm of the difference, stop, otherwise continue from step 2.

In step 2 we solve the eigenvalue problem by a 2-dimensional spectral method, using Chebyshev differentiation in the directions of r and θ . In step 3, the eigenfunctions at the first iteration are labelled by the usual l, m and n quantum numbers, though with $m = 0$ for axisymmetry. The idea is to choose one and run through the iteration, hoping for convergence. When the method converges, we do obtain a stationary state but we do not arrive at a one-to-one correspondence between solutions of the starting linear problem and the final nonlinear problem.

For the energy eigenvalue E (which is not the conserved energy) we have the formula

$$E = \int |\nabla\psi|^2 + \phi|\psi|^2, \quad (9)$$

while the total angular momentum J^2 , after integration by parts, is :

$$J^2 = \int \left| \frac{\partial\psi}{\partial\theta} \right|^2 \quad (10)$$

Both integrals are over \mathbf{R}^3 .

We present in Table 1 the first few stationary states of the axially symmetric solution of the SN equations ordered by their energy and named for convenience axi1 to axi8.

In this table, axi1, axi3 and axi8 are spherically-symmetric solutions turning up again (as they should). Axi2, shown as a surface in figure 8 and as a contour plot in figure 9, is very much like a dipole solution and appears to be the solution minimising the energy among wavefunctions odd in z . If so

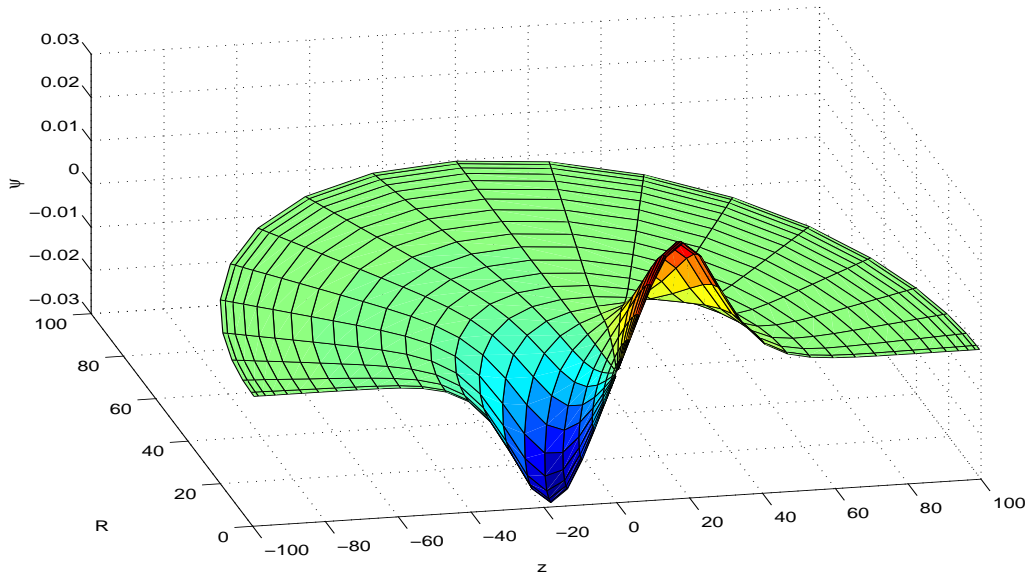


Figure 8: The dipole-like state, axi2.

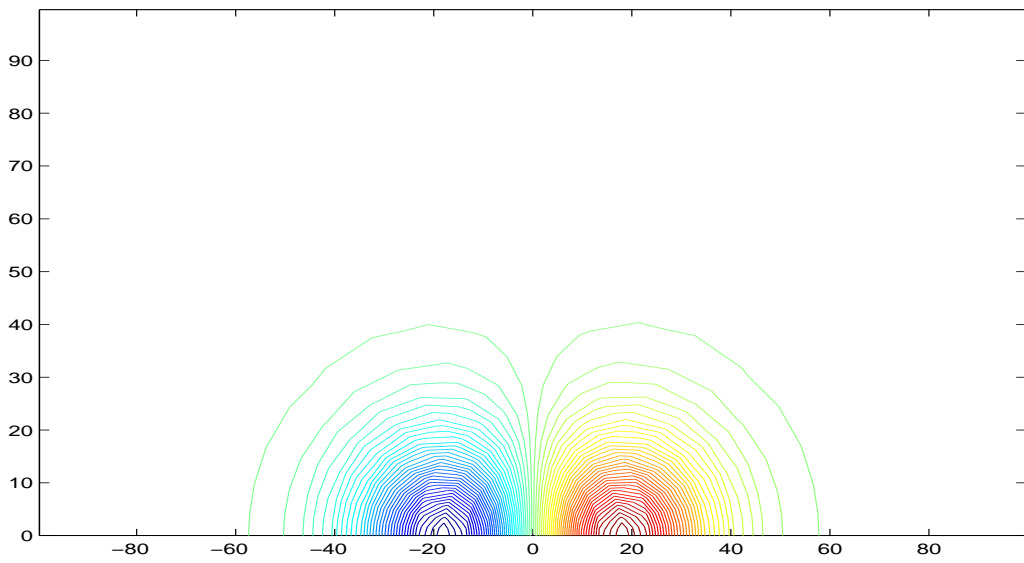


Figure 9: Contour Plot of the dipole, axi2.

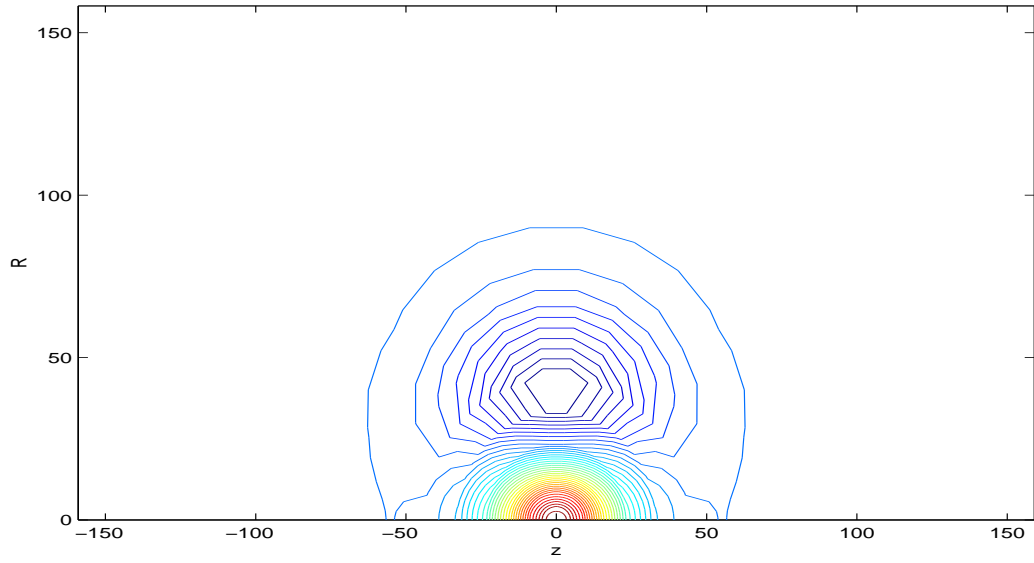


Figure 10: Contour plot of the state axi4.

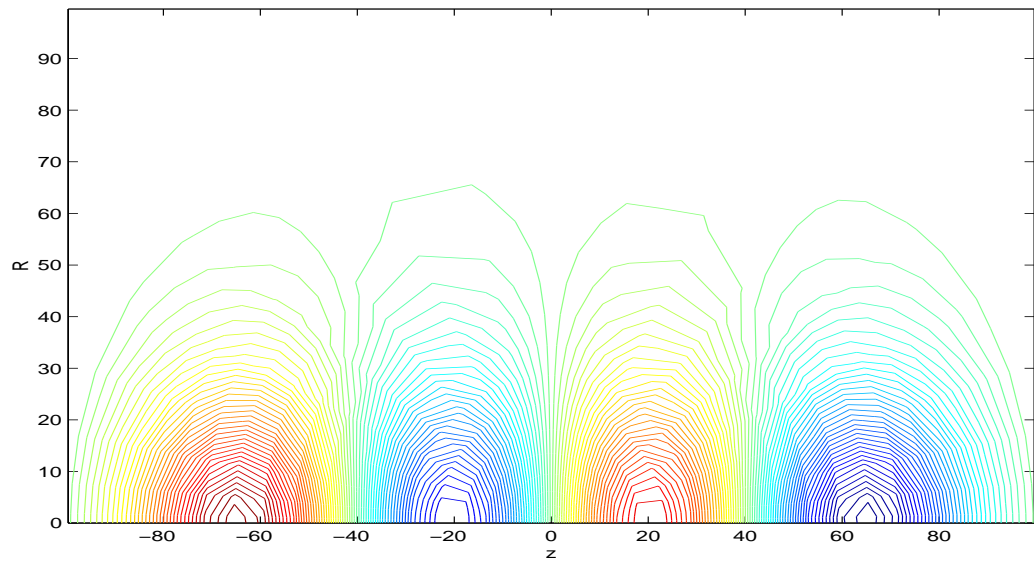


Figure 11: Contour plot of the state axi5.

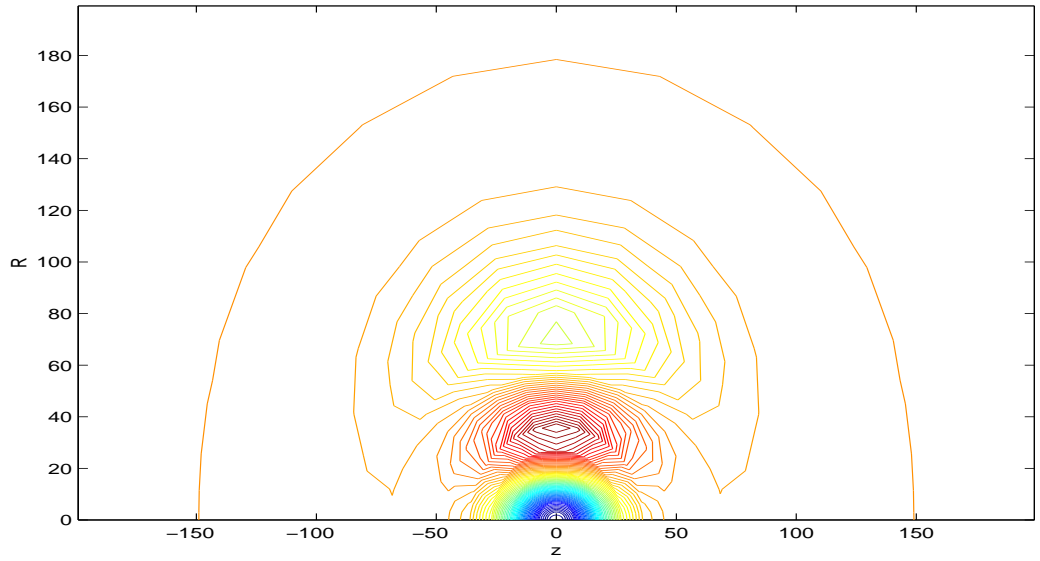


Figure 12: Contour plot of the state axis6.

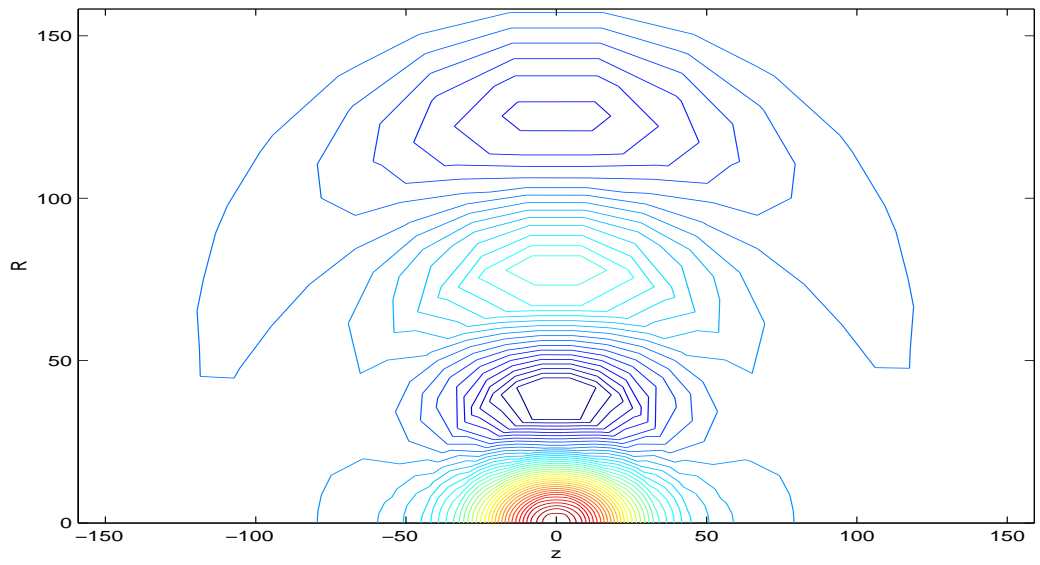


Figure 13: Contour plot of the state axis7.

| Energy | J^2 | name |
|---------|--------|------|
| -0.1592 | zero | axi1 |
| -0.0599 | 5.1853 | axi2 |
| -0.0358 | 0.002 | axi3 |
| -0.0292 | 2.3548 | axi4 |
| -0.0263 | 17.155 | axi5 |
| -0.0208 | 3.1178 | axi6 |
| -0.0162 | 5.2053 | axi7 |
| -0.0115 | 1.9E-6 | axi8 |

Table 1: The first few axially-symmetric stationary states.

it was found already in [9]. Contour plots of axi4-axi7 are given in figures 10 to 13.

To solve the time-dependent axisymmetric SN-equations, we shall use an alternating direction implicit (or ADI) method (see e.g.[1], [3] or [7]) We split the Laplacian in (7) to write it as

$$\dot{u} = i(L_1 + L_2 - \phi)u \quad (11)$$

where

$$L_1 = \frac{1}{r} \frac{\partial^2}{\partial r^2} \quad (12)$$

$$L_2 = \frac{1}{r} \left[\frac{\partial^2}{\partial \theta^2} + \cot \theta \frac{\partial}{\partial \theta} \right]. \quad (13)$$

Next we introduce new variables S and T and write this in the formally equivalent form:

$$\begin{aligned} \exp\left(-\frac{ih}{2}L_1\right)S(t) &= \exp\left(\frac{ih}{2}L_2\right)u(t) \\ \exp\left(-\frac{ih}{2}L_2\right)T(t) &= \exp\left(\frac{ih}{2}L_1\right)S(t) \\ \exp\left(\frac{ih}{2}\phi\right)u(t+h) &= \exp\left(-\frac{ih}{2}\phi\right)T(t) \end{aligned} \quad (14)$$

where we suppress the dependence on r and θ . To obtain a discrete form of (14) we linearise in the time-step h to find

$$\left(1 - \frac{ih}{2}L_1\right)S^n = \left(1 + \frac{ih}{2}L_2\right)u^n$$

$$\begin{aligned}
(1 - \frac{ih}{2}L_2)T^n &= (1 + \frac{ih}{2}L_1)S^n \\
(1 + \frac{ih}{2}\phi^{n+1})u^{n+1} &= (1 - \frac{ih}{2}\phi^n)T^n
\end{aligned}
\tag{15}$$

where the superscript indicates the value of discretised time.

For the Poisson equation (8) we have

$$(L_1 + L_2)(r\phi) = \frac{1}{r^2}|u|^2$$

which we solve at each instant by a Peaceman-Rachford ADI iteration [1]. This means we discretise it as

$$\begin{aligned}
(L_1 + \rho)\phi_{k+1} &= -(L_2 - \rho)\phi_k + \frac{1}{r^2}|u|^2 \\
(L_2 + \rho)\phi_{k+1} &= -(L_1 - \rho)\phi_k + \frac{1}{r^2}|u|^2
\end{aligned}
\tag{16}$$

and iterate with $\phi^0 = 0$. Here k labels the iteration (at a fixed time) and ρ is a small constant chosen so that the iteration converges.

The boundary conditions are that u and ϕ vanish at the outer boundary and so we need sponges as in Section 2 to prevent waves of probability reflecting back.

As an example, we take as initial data the dipole state of figure 8. The evolution of $|\psi|$ for this is shown in figure 14. (Note that ψ is initially real but must become complex before again becoming approximately real in the remote future. The initial data for ψ is odd as a function of z but it ends up approximately even.)

Following the lessons learned in Section 3, we should expect the stationary state to be unstable. We can compute the evolution for short times to see that initially it remains a stationary state, that is that the only change is a phase growing linearly with time. However when numerical errors have built up the state becomes unstable and the two concentrations of probability density fall into each other. Probability leaves the grid, as does angular momentum, and we are left with a multiple of the ground state. We can check convergence of the method by calculating a Richardson quotient with three different time-steps (to find that convergence is now linear in time), and by varying the number of Chebyshev points.

What we learn from this calculation is that, as well as dispersion which is what we mostly saw in Section 3, the solutions of the SN equation show

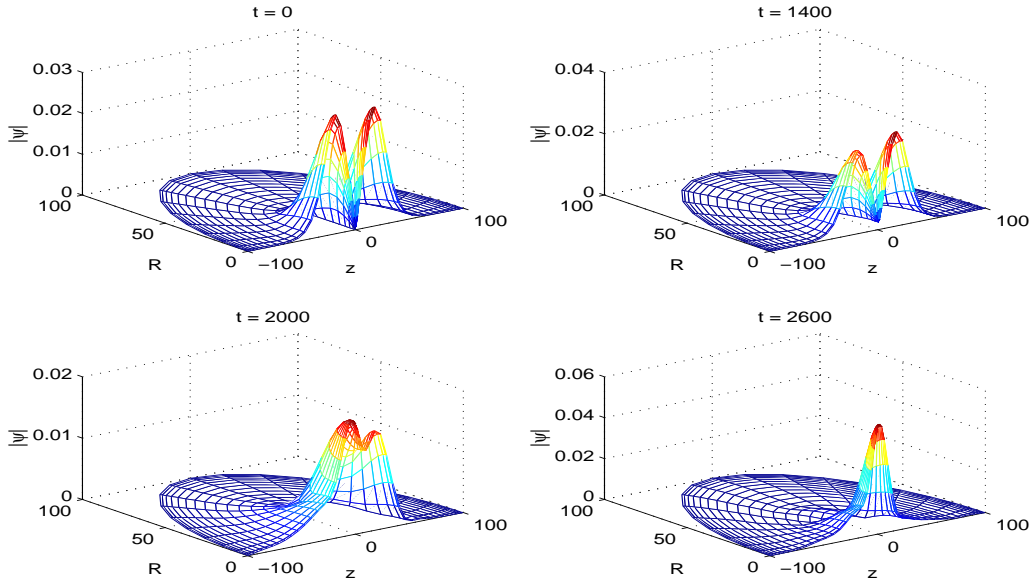


Figure 14: Evolution of the dipole.

gravitational attraction: lumps of probability density released from rest fall into each other. In the next section we shall see that, at least for the two-dimensional SN equations, lumps of probability can orbit each other.

5 The two-Dimensional SN equations

In this section, we shall consider the SN equations in a plane, that is in Cartesian coordinates x, y . We shall find a dipole-like stationary solution, and some solutions which are like rigidly rotating dipoles. These rigidly rotating solutions are unstable however and will merge, radiating angular momentum.

The SN equations in this case are

$$\begin{aligned} i\psi_t &= -\psi_{xx} - \psi_{yy} + \phi\psi \\ \phi_{xx} + \phi_{yy} &= |\psi|^2 \end{aligned} \tag{17}$$

We use the ADI scheme as in equation (15) but with the understanding that now

$$L_1 = \frac{\partial^2}{\partial x^2}$$

$$L_2 = \frac{\partial^2}{\partial y^2}.$$

For the potential we use the counterpart of (16) with the same understanding. The boundary conditions are that ψ and ϕ vanish at the edges of the grid, which is now a large square. We still need sponges and we do not want them to have corners so we take functions like $s(x, y) = \min[1, e^{0.5(\sqrt{x^2+y^2}-20)}]$. We can test the efficacy of the sponges by evolving moving two-dimensional Gaussians to see that they propagate off the grid, as they do.

Once we have the code, we can look for solutions corresponding to those found already in 3-dimensions. In particular we find a stable ground state and a dipole-like solution which is stable for a while before decaying to the ground state. We can seek solutions with no counterpart among those found already by making an ansatz of rigid rotation. That is we look for solutions which in polar coordinates r, θ take the form:

$$\psi(r, \theta, t) = e^{-iEt}\psi(r, \theta + \omega t) \quad (18)$$

for (real) constants E and ω . (Solutions of a similar nature in 3-dimensions would depend on all three spatial coordinates which is why we haven't seen them so far.)

To separate the SN equations for a solution like (18), we go into the rotating frame with Cartesian coordinates X, Y given by

$$\begin{aligned} X &= x \cos \omega t + y \sin \omega t, \\ Y &= -x \sin \omega t + y \cos \omega t, \end{aligned}$$

and the time-dependence separates off to leave the equations as

$$\begin{aligned} -\nabla^2\psi + \phi\psi - i\omega(Y\psi_X - X\psi_Y) &= E\psi \\ \nabla^2\phi &= |\psi|^2, \end{aligned} \quad (19)$$

To solve (19), we begin with a small value of ω and the dipole-like solution. Iteration leads to a solution, and we can study its change with increasing ω . The wave-function ψ is necessarily complex and we display the real and imaginary parts of such a solution, with $\omega = 0.005$, in figures 15 and 16.

The solution just found is a stationary state but we must expect it to be unstable. If we use it as initial data for the time-dependent problem then we find as before that it evolves as a stationary state for some time (see figure 17)

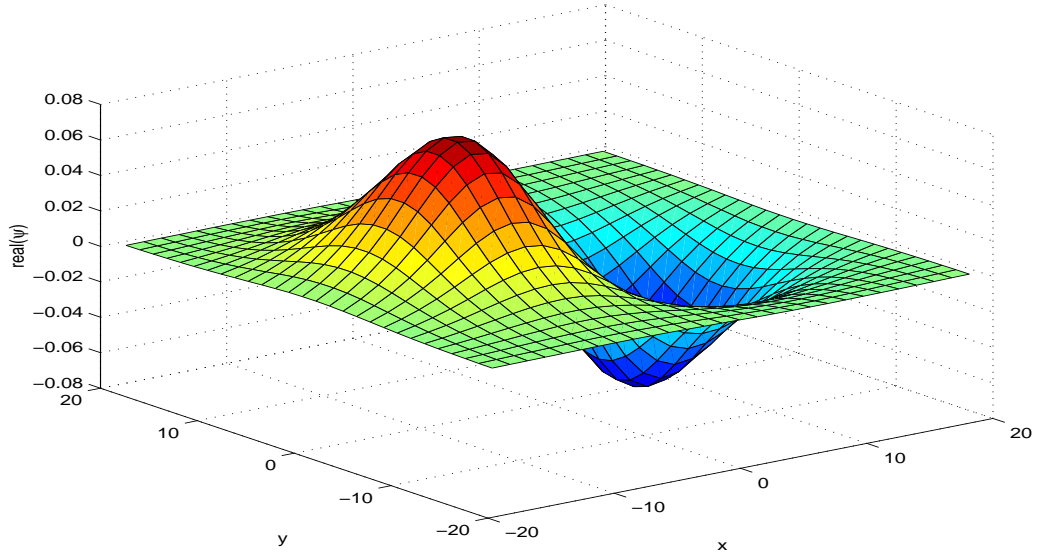


Figure 15: Real part of spinning solution, $\omega = 0.005$.

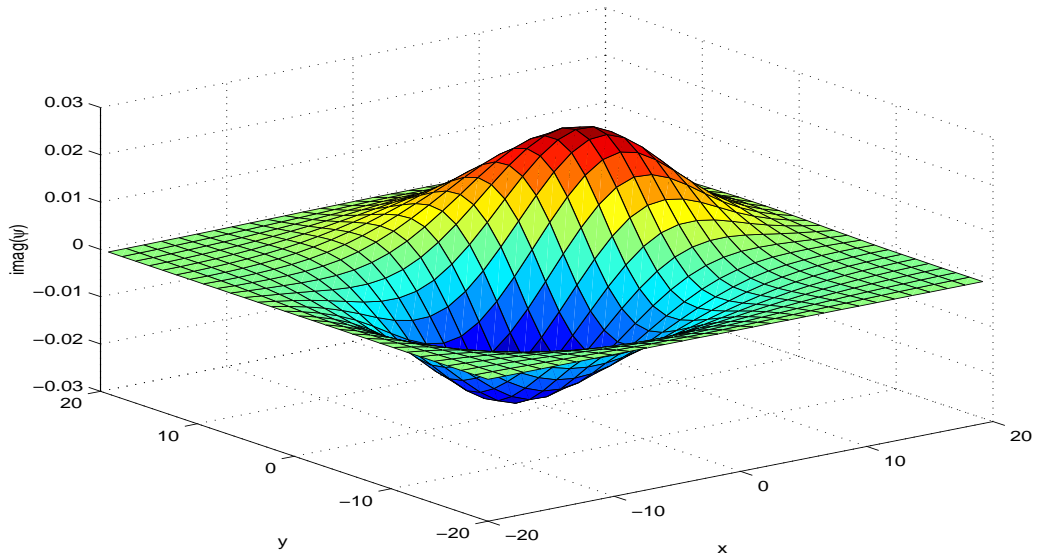


Figure 16: Imaginary part of spinning solution, $\omega = 0.005$.

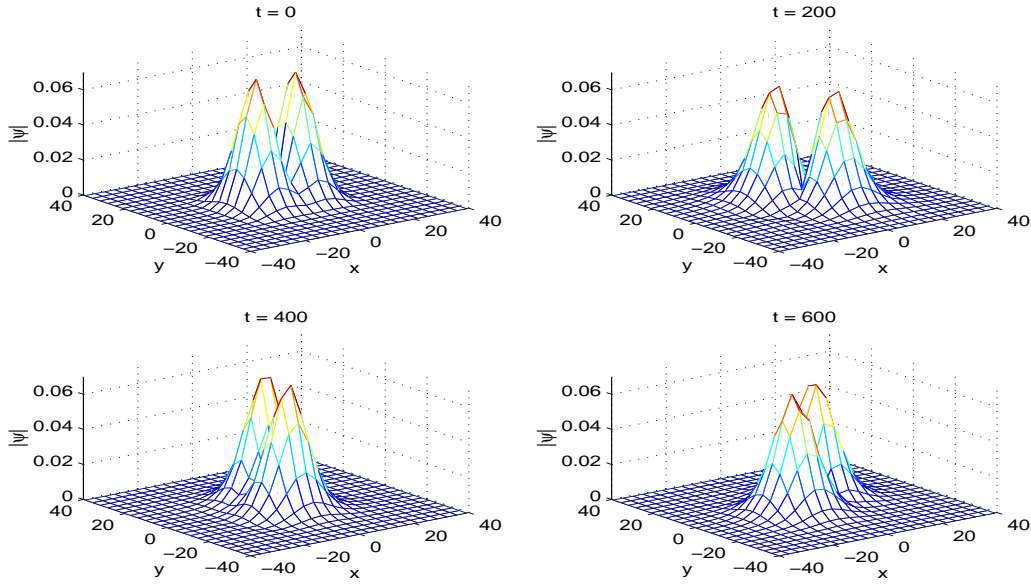


Figure 17: Initial evolution of spinning solution: orbiting.

before numerical errors build up and it becomes unstable (figure 18). The two lumps of probability orbit each other about four times before collapsing into a single lump in about one orbital period. Probability and angular momentum are radiated off of the grid.

What we have found by this calculation is a confirmation of the picture of lumps of probability interacting gravitationally with each other. Here the lumps are in orbit around each other for a while before becoming unstable and collapsing into a single lump. By earlier work, we must then expect the probability to disperse leaving a rescaled ground state, as it does.

Acknowledgement

The work described in this paper formed part of the D.Phil. thesis of the first author and he gratefully acknowledges the receipt of a grant from EPSRC.

References

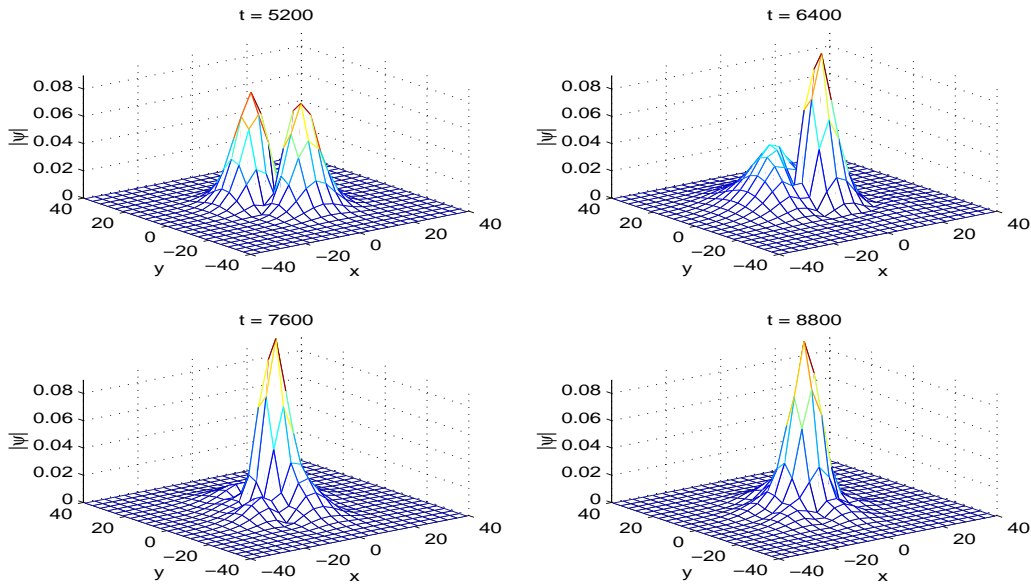


Figure 18: Later evolution of spinning solution: collapse.

- [1] W.F.Ames, “Numerical Methods for Partial Differential Equations” 2nd ed, Academic Press: Boston (1977)
- [2] D.H.Bernstein, E.Giladi and K.R.W.Jones, Eigenstates of the Gravitational Schrödinger Equation, *Modern Physics Letters* **A13** (1998) 2327-2336
- [3] R.Guenther, A numerical study of the time dependent Schrödinger equation coupled with Newtonian gravity, unpublished Ph.D. thesis, University of Texas at Austin (1995).
- [4] R.Harrison, I.Moroz and K.P.Tod, A numerical study of the Schrödinger-Newton equations 1: Perturbing the spherically-symmetric stationary states, in preparation (2001)
- [5] I.M.Moroz and K.P.Tod, An Analytical Approach to the Schrödinger-Newton equations, *Nonlinearity* **12** (1999) 201-16
- [6] I.M.Moroz, R.Penrose and K.P.Tod, Spherically-symmetric solutions of the Schrödinger-Newton equations, *Class Quantum Grav.* **15** (1998) 2733-2742

- [7] K.W.Morton and D.F.Mayers “Numerical solution of partial differential equations”, CUP: Cambridge (1994)
- [8] R.Ruffini and S.Bonazzola, Systems of Self-Gravitating Particles in General Relativity and the concept of an Equation of State, *Phys.Rev.***187** (1969) 1767
- [9] B.Schupp, J.J. van der Bij, An axially-symmetric Newtonian boson star, *Phys. Lett. B* **366** (1996) 85-88
- [10] K.P.Tod, The ground state energy of the Schrödinger-Newton equations, *Phys.Lett.A* **280** (2001) 173-176